PCCP

COMMUNICATION

View Article Online
View Journal | View Issue

Enhancing electron transport in molecular wires by insertion of a ferrocene center†

Cite this: *Phys. Chem. Chem. Phys.*, 2014, **16**, 2260

Received 1st August 2013,
Accepted 11th November 2013

DOI: 10.1039/c3cp53269k

www.rsc.org/pccp

Yan-Yan Sun,[a] Zheng-Lian Peng,[a] Rong Hou,[b] Jing-Hong Liang,[c] Ju-Fang Zheng,[a] Xiao-Yi Zhou,[a] Xiao-Shun Zhou,*[a] Shan Jin,*[b] Zhen-Jiang Niu[a] and Bing-Wei Mao[c]

We have determined the conductance of alkane-linked ferrocene molecules with carboxylic acid anchoring groups using the STM break junction technique, and three sets of conductance values were found, *i.e.* high conductance (HC), medium conductance (MC) and low conductance (LC) values. The enhancing effect of the incorporated ferrocene on the electron transport in saturated alkane molecular wires is demonstrated by the increased conductance of the ferrocene molecules, attributed to the reduction of the tunneling barrier and the HOMO–LUMO gap induced by the insertion of ferrocene. Furthermore, the electron-withdrawing carbonyl group on the unconjugated backbone has little or no influence on single-molecule conductance. The current work provides a feasible approach for the design of high-performance molecular wires.

Introduction

The goal of molecular electronics is to facilitate the manufacturing of electronic devices from single molecules.[1–4] In particular, linear single molecules with two anchoring groups have received great attention, as they can serve as rectifiers,[5–7] switches,[8,9] transistors,[10–12] wires,[13–15] and other key electronic components.[16] It is crucially important to measure and effectively control the electron transport through single molecules for the purpose of developing molecular electronic devices. A promising approach to examine the electron transport behavior of single molecules is to construct metal–molecule–metal junctions and measure their single molecular conductance. Therefore, various technologies were developed, including STM break junction (STM-BJ),[14,17–21] mechanically controllable break junction (MCBJ),[19,22–24] conducting atomic force microscopy (C-AFM),[25–27] STM trapping method[28] and electromigration.[29–31] Studies have shown that the electron transport through single-molecule junctions is strongly affected by the intrinsic nature of the molecular structures, the molecule–electrode contact and the local environment of the molecule.[16,32,33] The intrinsic nature of the molecule includes the degree of electronic delocalization,[34] substituent groups,[35,36] and molecular topology.[18] Recently, molecules with redox centers have received increasing attention, as the electron transport in such molecular junctions can be reversibly tuned by a gate electrode (or electrochemical gate). To date, many devices comprising redox centers as controllable switches or transistors have been reported, including viologens,[37,38] metal transition complexes,[21,39] perylenetetracarboxylic diimide derivatives,[11] terathiafulvalenes,[12,40] ferrocene,[41] anthraquinone,[9,42] perylenetetracarboxylic bisimide,[43] and redox-active proteins.[44,45] However, a few works have been done to assess the enhancing effect of the redox center on the electron transport behavior of single-molecule junctions.[42,46–48]

Ferrocene molecules are possibly the earliest and most widely studied redox molecules due to their satisfactory electrochemical reversibility and synthetic stability.[49] For example, many ferrocene-based molecular devices have been studied, including molecular wires,[47] transistors,[31,50] rectifiers,[7,51] and negatively differential resistance devices.[52,53] Compared with compounds with a thioacetyl terminal group, linear compounds with carboxylic terminal groups can be easily synthesized with high yields and chemical stability. We report here a study on the electron transport in alkane-linked ferrocene molecules with carboxylic acid anchoring groups (Fig. 1), with a particular focus on the effect of the inserted ferrocene center and electron-withdrawing carbonyl groups on the electron transport characteristics of a saturated alkane.

[a] *Zhejiang Key Laboratory for Reactive Chemistry on Solid Surfaces, Institute of Physical Chemistry, Zhejiang Normal University, Jinhua, Zhejiang 321004, P. R. China. E-mail: xszhou@zjnu.edu.cn*
[b] *Key Laboratory of Pesticide & Chemical Biology of the Ministry of Education, College of Chemistry, Central China Normal University, Wuhan 430079, P. R. China. E-mail: jinshan@mail.ccnu.edu.cn*
[c] *State Key Laboratory for Physical Chemistry of Solid Surfaces and Chemistry Department, College of Chemistry and Chemical Engineering, Xiamen University, Xiamen, Fujian 361005, P. R. China*

† Electronic supplementary information (ESI) available: Conductance histograms for 1,4-phenylenedipropionic acid and the HOMO and LUMO energy levels and orbitals of molecules. See DOI: 10.1039/c3cp53269k

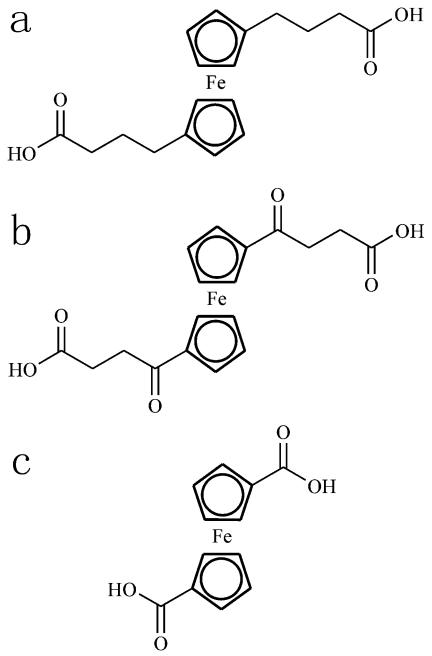

Fig. 1 Molecular structure of the ferrocene molecules: (a) Fc-1, (b) Fc-2 and (c) Fc-3.

Experimental section

Reagents

Ferrocene molecules were prepared according to the literature procedures.[49,54] The ferrocene center is very stable in air and adopts the +2 oxidation state in these molecules.[49] 1,6-Hexanedicarboxylic acid was purchased from Alfa Aesar, while terephthalic acid and 1,4-phenylenedipropionic acid were purchased from Sigma-Aldrich. All aqueous solutions were prepared with ultrapure water (>18 MΩ cm).

Adsorption

Au(111) was immersed in freshly prepared dichloromethane or acetone solutions containing 0.1 mM target ferrocene molecules for 5 min and then in dichloromethane or acetone solvent for 5 min. The naturally formed (111) facet of the single crystal beads was used for the conductance measurement, while Au(111) from Mateck was used for cyclic voltammetry.

Characterization

Cyclic voltammetry (CV) was performed on a CHI 660D electrochemical workstation in a three-electrode electrochemical cell with an SCE reference electrode and a Pt counter electrode. Conductance measurements were carried out on a modified Nanoscope IIIa STM (Veeco, US) with external control of the z-piezo movement in ambient conditions.[21,55,56] Briefly, the electrochemically etched Au tip was driven toward and out of contact with the molecule-adsorbed Au(111) substrate at a fixed bias. Then the tip current was recorded at a sampling frequency of 20 kHz during the pulling of the tip away from the Au(111) at a typical speed of 20 nm s^{-1}. This process was repeatedly performed until enough data for a large number of conductance–distance curves had been collected.[17] The curves with clear stepwise features were selected to make the histogram (the ratios for the data selection was around 15%).

Results and discussion

CV and conductance measurements of Fc-1

CV characterizations of self-assembled monolayer (SAM) of the three molecules on Au(111) electrodes were carried out in 0.1 M H_2SO_4 aqueous solution. As shown in Fig. 2a, a pair of well-defined reversible peaks for Fc-1 was observed at *ca.* 0.5 V *vs.* SCE. As expected for the voltammetric behavior of the surface-confined redox species, the redox peak current density is linearly proportional to the scan rate (Fig. 2b), demonstrating that Fc-1 was self-assembled onto the Au(111) surface. The surface coverage evaluated from the cyclic voltammetric reduction peak area was 3×10^{13} molecules cm^{-2}, which indicates that the surface coverage of Fc-1 on the gold electrode is less than a monolayer.[41] The STM image of Fc-1 adsorbed on Au(111) is shown in Fig. 2c. The CV and STM results clearly show that Fc-1 has been successfully assembled on the Au(111).

The single-molecule conductance of Fc-1 was measured by STM-BJ under ambient conditions at room temperature. Fig. 3a shows the typical conductance traces with stepwise features at the bias voltage of 50 mV. The conductance histogram constructed from hundreds of curves with stepwise features produces a peak of preferential occurrence of conductance at 16 nS (inset of Fig. 3b). The two-dimensional (2D) conductance histogram was obtained

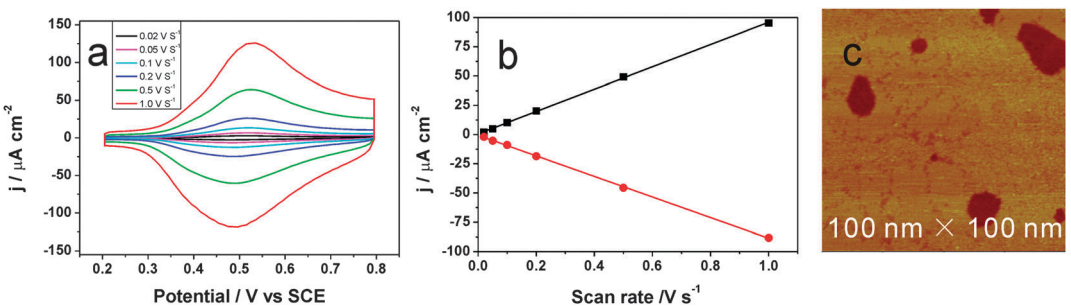

Fig. 2 (a) Cyclic voltammograms (CVs) of Fc-1 adsorbed onto Au(111) in 0.1 M H_2SO_4 aqueous solution with scan rates of 20, 50, 100, 200, 500, 1000 mV s^{-1}. (b) Linear dependency between the current density intensity of the anodic (black square) and cathodic (red circle) peaks and the scan rates. (c) Large-scale STM image (100 nm × 100 nm) of the SAM of Fc-1 on Au(111). E_{bias} = 465 mV, I_{tip} = 1.53 nA.

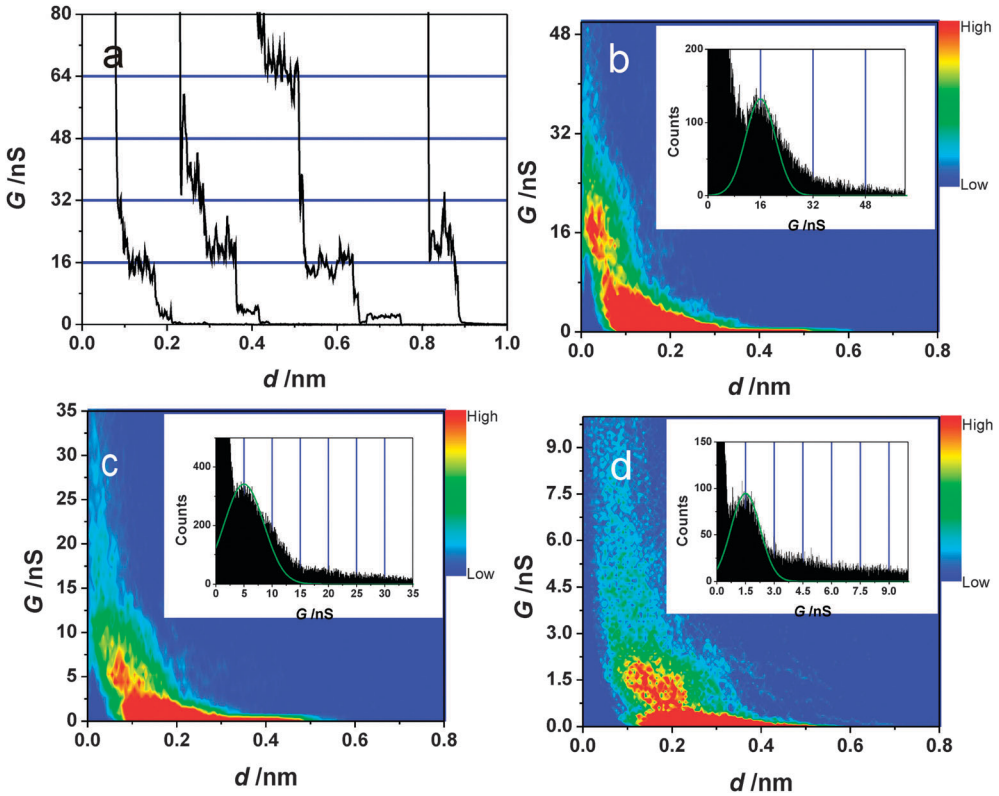

Fig. 3 (a) Typical conductance (G)-distance (d) traces and (b) conductance histogram of the single-molecule junction of Fc-1 with a high conductance value. Two-dimensional histograms of (c) medium conductance and (d) low conductance values of Fc-1. Insets are the corresponding conductance histograms. The conductance value of 190 nS was set as the zero distance for all three 2D histograms.

by counting the number of data points at each conductance value with each stretching distance from the conductance curves. The conductance value and typical step length of the molecular junctions can be obtained from the high counts of the 2D histogram. Typically, a special conductance value was set as the zero distance in each of the 2D histograms. Fig. 3b shows the same conductance value in the 2D histogram as that with the one-dimensional histogram method.

The step length measures the distance over which a molecular junction can be stretched before its conductance jumps to another step,[17] while the breaking-off length of single-molecule junctions represents the distance from the metal-to-metal point contact (77.4 μS for Au) to the end of the conductance plateau before the junction breaks in conductance *vs.* distance curves.[57] Coming back to our experiment, the typical step length of the conductance curves is around 0.1 nm, which is similar to that reported by Tao's group[58] and Nichols' group[57] using the same carboxylic acid group. However, this value is much less than the length of Fc-1 (1.6 nm). The reason is that the step length may be caused by the slip of the COO^- or Au atom on the electrode, and does not represent the molecule length. Interestingly, the breaking-off length is comparable to the length of the molecule reported by Nichols's group.[57] However, the peak is centered on a very low distance in Fig. 3, which is caused by the fact that the zero distance is not the metal-to-metal point contact.

Besides the conductance value of 16 nS, the steps with values of ~5 nS and ~1.5 nS can also be often obtained from conductance curves. For example, the step value of ~5 nS can be found in the second curve of Fig. 3a, while the step value of ~1.5 nS can be seen in the third curve of Fig. 3a. Here, we defined the three sets of conductance values 16 nS (Fig. 3b), 5 nS (Fig. 3c) and 1.5 nS (Fig. 3d) as high conductance (HC), medium conductance (MC) and low conductance (LC) values, respectively. Moreover, three sets of conductance values can also be obtained in one histogram as shown in Fig. 4, though the shape of the third peak is not so good and has a small shift value. The HC is about 3 times that of the MC, while the MC is about 3 times of the LC. The ratios among HC, MC and LC are similar to that of 4,4′-(ethane-1,2-diyl)dibenzoic acid with the same anchoring group reported by Martin *et al.*[57] In addition, multiple sets of conductance values were also reported for the other anchoring groups, such as thiol, pyridyl and amine,[19,58–61] and can be attributed to different contact geometries between the anchoring group and the electrodes.[57,58]

The influence of the substituent group on the unconjugated backbone

In order to investigate the influence of the substituent on the backbone, the conductance of Fc-2 with a carbonyl group on the backbone was determined. The conductance histograms are shown in Fig. 5. There are also three sets of conductance

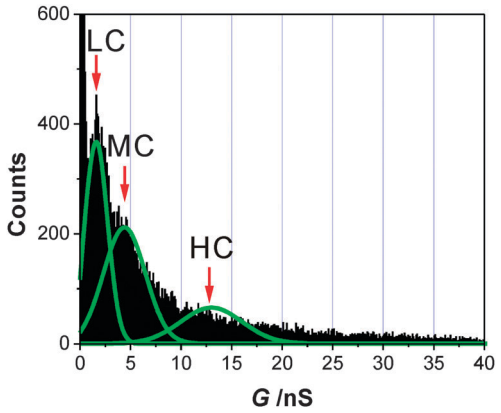

Fig. 4 The conductance histogram of Fc-1 shows the HC, MC and LC values.

values, *i.e.* the HC, MC and LC are 16 nS, 5 nS and 1.5 nS, respectively. Interestingly, these values are almost the same as those of Fc-1, which indicates that the electron-withdrawing carbonyl group has little effect on the conductance. A similar result was reported for glycine and alanine, and there is one more methyl substituent on the backbone for alanine.[62] According to previous literature reports, the molecular conductance depends on the substituent,[35,36] and attachment of an electron-donating substituent would raise the energy levels of the frontier molecular orbital, while an electron-withdrawing substituent would lower those energy levels. Therefore, the energy separation between the frontier molecular levels and E_{fermi} of the metal electrode can be changed, which would alter the single-molecule conductance.

We have carried out DFT SIESTA code calculations[63,64] for the HOMO and LUMO levels of Fc-1 and Fc-2. The energies of the HOMO and LUMO are −4.22 eV and −1.48 eV (HOMO–LUMO gap 2.74 eV) for Fc-1, and −4.55 eV and −2.1 eV (HOMO–LUMO gap 2.45 eV) for Fc-2, respectively. These results indicate that the attachment of the electron-withdrawing carbonyl group lowers the frontier molecular levels. Interestingly, the absence of a substituent effect is found in the conductance measurements. To better understand this phenomenon, further theoretical investigation on the contributions from each of the molecular conductance orbitals is therefore needed.

The influence of the molecule length on the conductance

The length dependence of the single-molecule conductance was also carried out by the conductance measurement of Fc-3 with the shorter length. As shown in Fig. 6, there are three sets of single-molecule conductance values, which are 480 nS (HC), 160 nS (MC) and 60 nS (LC). The HC is about 3 times that of the MC, while the MC is about 3 times of the LC. For Fc-3, the conductance value is about 30 times that of Fc-1 which terminates with $-(CH_2)_3-$ units at both ends of the ferrocene center compared with Fc-3. Xiao *et al.* also reported that the conductance value of cysteamine–ferrocene–cysteamine is about 5 times that of cysteamine–Gly–ferrocene–Gly–cysteamine, which also have one more $-CH_2-NH-CH_2-$ unit at both ends compared with cysteamine–ferrocene–cysteamine.[41] The different ratio may due to the following reason: there is similar electron coupling between cysteamine–ferrocene–cysteamine and cysteamine–Gly–ferrocene–Gly–cysteamine; compared with Fc-3, the insertion of two $-(CH_2)_3-$ groups would destroy the electron coupling of Fc-1, leading to a more remarkable decrease in conductance.

Enhancing molecular conductance by insertion of ferrocene

Now we will focus on the influence on conductance by the ferrocene center. The single-molecule conductance of 1,6-hexanedicarboxylic acid (HOOC–C6–COOH) was first measured. As shown in Fig. 7, 1,6-hexanedicarboxylic acid has conductance values of 2.8 nS, 0.8 nS and 0.28 nS for the HC, MC and LC, respectively. These values are in agreement with previous reports of Chen *et al.*[58] and Martin *et al.*[65] Though Fc-1 (HOOC–C3–Fc–C3–COOH with a length of 1.6 nm) is longer than 1,6-hexanedicarboxylic acid (HOOC–C6–COOH with a length of 1.1 nm), Fc-1 is more conductive. Taking the HC value of single-molecule conductance as an example, the single-molecule conductance of Fc-1 is 16 nS, and about 6 times that of 1,6-hexanedicarboxylic acid. This result illustrates that ferrocene can be utilized to enhance the electron transport ability of a molecular wire by insertion into a molecular wire. Moreover, conductance measurements of 1,4-phenylenedipropionic acid give rise to conductance values of 17 nS, 5.5 nS and 1.6 nS for the HC, MC and LC, respectively, as shown in Fig. S1 (ESI†). Hence, the conductance values of Fc-1 (16 nS, 5 nS, and 1.5 nS) are similar to those for 1,4-phenylenedipropionic acid, which has a phenyl group center and an even

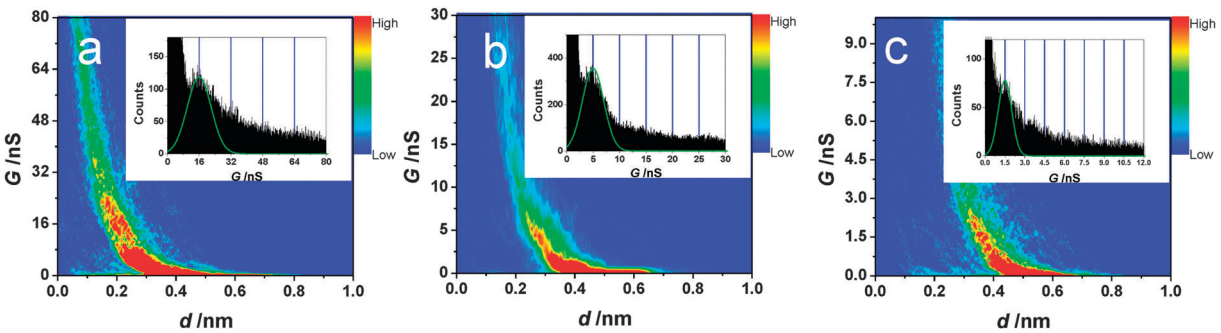

Fig. 5 Two-dimensional histograms of the (a) HC, (b) MC and (c) LC values of Fc-2. Insets are the corresponding conductance histograms. The conductance value of 190 nS was set as the zero distance for all three 2D histograms.

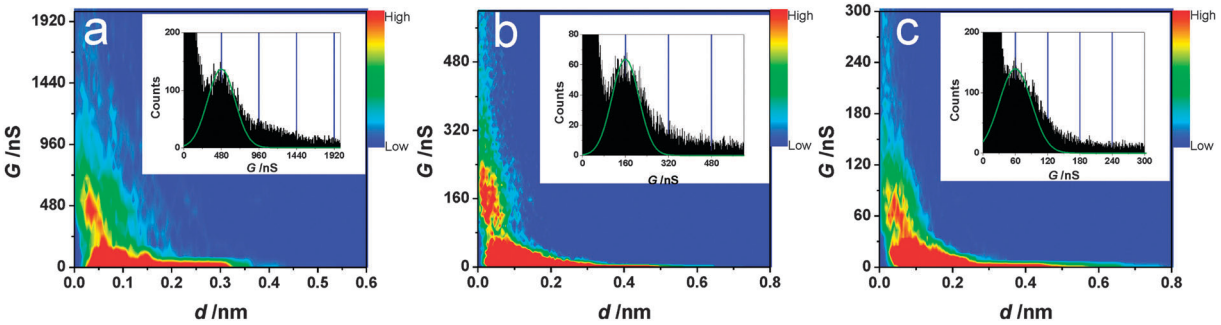

Fig. 6 Two-dimensional histograms of the (a) HC, (b) MC and (c) LC values of Fc-3. Insets are the corresponding conductance histograms. The conductance value of 19 000 nS was set as the zero distance for the HC histogram, and 1900 nS was set as the zero distance for the MC and LC histograms.

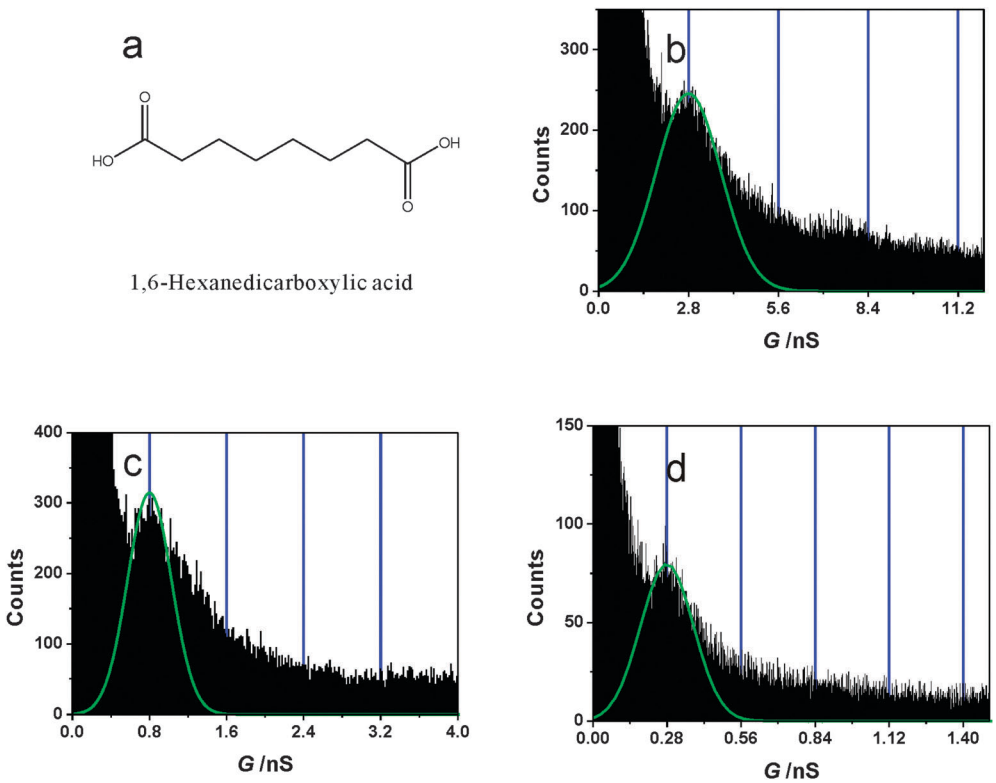

Fig. 7 (a) Structure of 1,6-hexanedicarboxylic acid. One-dimensional histograms of (b) the HC, (c) MC and (d) LC values of 1,6-hexanedicarboxylic acid.

shorter length (missing one $-CH_2-$ at both ends) compared with Fc-1. These facts also demonstrate the enhancing effect on electron transfer by the ferrocene center.

It is unsuitable to compare the conductance value between Fc-3 (HOOC–Fc–COOH) and oxalic acid (HOOC–COOH), due to the existence of through-space electron transport in ultrashort molecular junctions.[33] Therefore, terephthalic acid (TPA) was chosen as a model molecule to compare with Fc-3. As shown in Fig. 8, three types of conductance values were observed with conductance of 250 nS, 90 nS and 30 nS for the HC, MC and LC, respectively. The single-molecule conductance of Fc-3 is about twice that of terephthalic acid (TPA), *i.e.* 480 nS, 160 nS and 60 nS for the HC, MC and LC of Fc-3, respectively. The ratio between conductance values of Fc-3 and TPA are similar to those values for molecules with thiol as the anchoring group reported by Lu *et al.*[47] The enhancement of the molecular conductance of Fc-3 can also be attributed to the reduced tunneling barrier (energy between the molecular HOMO level and the electrode Fermi level) in the junction.[47]

The above results demonstrate that the insertion of ferrocene can enhance molecular conductance. Similar results were also reported for other molecules with a redox center. For example, Wen *et al.* found that molecules with two ruthenium redox centers exhibit higher molecular conductance than that of oligo(*p*-phenylene ethynylene (OPE) with a similar length, which was ascribed to the better energy match of the Fermi level of the electrodes with

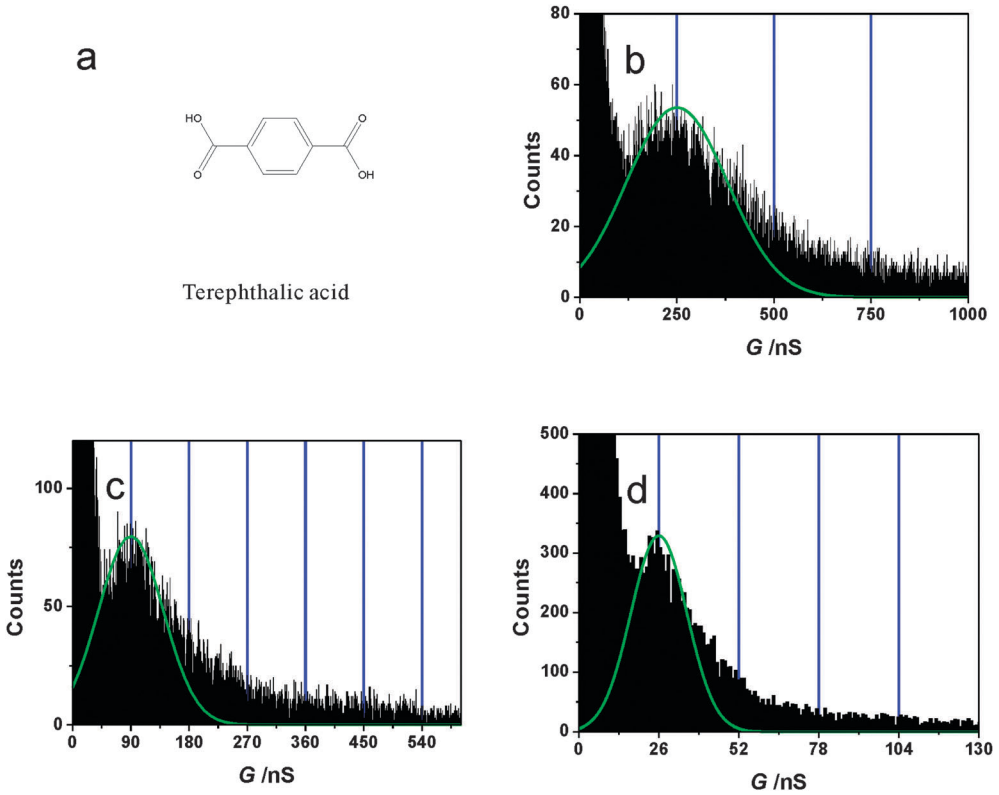

Fig. 8 (a) Structure of terephthalic acid. One-dimensional histograms of (b) the HC, (c) MC and (d) LC values of terephthalic acid.

the HOMO of the molecule having two ruthenium redox centers.[48] Also, Lu *et al.* reported that conjugated OPEs incorporating ferrocene would enhance the molecular conductance, which is attributable to the reduction of their tunneling barriers in the tunneling region.[47] In the above studies, molecules with different backbones were compared to investigate the influence of redox center, while direct conductance measurements and comparisons between the same backbone with or without a redox center were carried out in this work. Besides, it is reported that the conductance of dithiol benzene derivatives and the dithiol viologen molecule is greater than that of alkanedithiol with the same or shorter length by Nichols' group, and they explain that the benzene or bipyridinium provides an effective reduction in the tunneling barrier.[66,67]

Returning to the current molecules, the DFT SIESTA code calculations provide the HOMO and LUMO energy levels (Table S1, ESI†) and orbitals (Table S2, ESI†) of these molecules. The charge is mainly located at the ferrocene center for Fc-1, Fc-2 and Fc-3, while the charge spans across the molecular bridge for 1,6-hexanedicarboxylic acid and terephthalic acid. Assuming that the Au Fermi level is equal to the work function of −5.1 eV,[68] the molecular HOMO levels are closer to the Au Fermi level. One can expect that the transport is dominated by the molecular HOMO level in these molecules. The tunneling barrier defines the energy between the electrode Fermi level and molecular energy levels.[32] For Fc-1 and 1,6-hexanedicarboxylic acid, the tunneling barrier of Fc-1 is small. Similarly, the tunneling barrier of Fc-3 is less than that of terephthalic acid. These reveal that the enhanced molecular conductance by the insertion of ferrocene may be attributed to the reduced tunneling barrier in the junction. On the other hand, ferrocene molecules have a smaller HOMO–LUMO gap (less than 2.74 eV) than that of 1,6-hexanedicarboxylic acid (5.27 eV) and terephthalic acid (3.49 eV). The small HOMO–LUMO gap may also contribute to the high electron transport efficiency through the ferrocene molecules. Correspondingly, the enhanced molecular conductance by the insertion of ferrocene in the current work may be due to the influence of the redox center (ferrocene), which reduces the tunneling barrier and the HOMO–LUMO gap.[47] A two-step mechanism for the electron transport through the redox center is also proposed.[67,69] However, further experimental and theoretical investigations are needed to better understand the enhancing effect.

Conclusions

We have studied the single-molecule conductance of ferrocene-based molecules by the STM break junction technique. Three sets of conductance values were found for those molecules, which can be attributed to the different contact conformations between the anchoring group and electrode. The substituent group (carbonyl group) on the unconjugated backbone has little effect on the single-molecule conductance. Particularly, ferrocene has an enhancing effect on the electron transport in single-molecule junctions due to the reduction of the tunneling

barrier and the HOMO–LUMO gap. The current research reveals that molecular wires with excellent electron transport can be realized through the insertion of a redox center (such as ferrocene).

Acknowledgements

The authors gratefully thank the National Natural Science Foundation of China for financial support (No. 21003110, 21273204, 20803027 and 21173094).

Notes and references

1 A. Nitzan and M. A. Ratner, *Science*, 2003, **300**, 1384–1389.
2 R. F. Service, *Science*, 2001, **294**, 2442–2443.
3 A. Aviram and M. A. Ratner, *Chem. Phys. Lett.*, 1974, **29**, 277–283.
4 M. Kiguchi and S. Kaneko, *Phys. Chem. Chem. Phys.*, 2013, **15**, 2253–2267.
5 S.-C. Chang, Z. Li, C. N. Lau, B. Larade and R. S. Williams, *Appl. Phys. Lett.*, 2003, **83**, 3198–3200.
6 J. Zhao, C. G. Zeng, X. Cheng, K. D. Wang, G. W. Wang, J. L. Yang, J. G. Hou and Q. S. Zhu, *Phys. Rev. Lett.*, 2005, **95**, 045502.
7 C. A. Nijhuis, W. F. Reus, A. C. Siegel and G. M. Whitesides, *J. Am. Chem. Soc.*, 2011, **133**, 15397–15411.
8 W. Nicolas, M. Artem, W. Thomas, N. Markus, L. Yann and M. Marcel, *Eur. J. Org. Chem.*, 2009, 6140–6150.
9 N. Darwish, I. Diez-Perez, P. Da Silva, N. J. Tao, J. J. Gooding and M. N. Paddon-Row, *Angew. Chem., Int. Ed.*, 2012, **51**, 3203–3206.
10 H. Song, Y. Kim, Y. H. Jang, H. Jeong, M. A. Reed and T. Lee, *Nature*, 2009, **462**, 1039–1043.
11 X. L. Li, J. Hihath, F. Chen, T. Masuda, L. Zang and N. J. Tao, *J. Am. Chem. Soc.*, 2007, **129**, 11535–11542.
12 N. J. Kay, S. J. Higgins, J. O. Jeppesen, E. Leary, J. Lycoops, J. Ulstrup and R. J. Nichols, *J. Am. Chem. Soc.*, 2012, **134**, 16817–16826.
13 S. Ho Choi, B. Kim and C. D. Frisbie, *Science*, 2008, **320**, 1482–1486.
14 G. Sedghi, V. M. Garcia-Suarez, L. J. Esdaile, H. L. Anderson, C. J. Lambert, S. Martin, D. Bethell, S. J. Higgins, M. Elliott, N. Bennett, J. E. Macdonald and R. J. Nichols, *Nat. Nanotechnol.*, 2011, **6**, 517–523.
15 D. K. James and J. M. Tour, *Top. Curr. Chem.*, 2005, **257**, 33–62.
16 N. J. Tao, *Nat. Nanotechnol.*, 2006, **1**, 173–181.
17 B. Q. Xu and N. J. Tao, *Science*, 2003, **301**, 1221–1223.
18 L. Venkataraman, J. E. Klare, C. Nuckolls, M. S. Hybertsen and M. L. Steigerwald, *Nature*, 2006, **442**, 904–907.
19 W. Hong, D. Z. Manrique, P. Moreno-García, M. Gulcur, A. Mishchenko, C. J. Lambert, M. R. Bryce and T. Wandlowski, *J. Am. Chem. Soc.*, 2012, **134**, 2292–2304.
20 M. Tsutsui, M. Taniguchi, K. Shoji, K. Yokota and T. Kawai, *Nanoscale*, 2009, **1**, 164–170.
21 X. S. Zhou, L. Liu, P. Fortgang, A. S. Lefevre, A. Serra-Muns, N. Raouafi, C. Amatore, B. W. Mao, E. Maisonhaute and B. Schöllhorn, *J. Am. Chem. Soc.*, 2011, **133**, 7509–7516.
22 C. A. Martin, D. Ding, J. K. Sorensen, T. Bjornholm, J. M. van Ruitenbeek and H. S. J. van der Zant, *J. Am. Chem. Soc.*, 2008, **130**, 13198–13199.
23 J. H. Tian, Y. Yang, B. Liu, B. Schollhorn, D. Y. Wu, E. Maisonhaute, A. S. Muns, Y. Chen, C. Amatore, N. J. Tao and Z. Q. Tian, *Nanotechnology*, 2010, **21**, 274012.
24 M. Taniguchi, M. Tsutsui, K. Yokota and T. Kawai, *Nanotechnology*, 2009, **20**, 434008.
25 B. Q. Xu, X. Y. Xiao and N. J. Tao, *J. Am. Chem. Soc.*, 2003, **125**, 16164–16165.
26 X. D. Cui, A. Primak, X. Zarate, J. Tomfohr, O. F. Sankey, A. L. Moore, T. A. Moore, D. Gust, G. Harris and S. M. Lindsay, *Science*, 2001, **294**, 571–574.
27 C. Nef, P. L. T. M. Frederix, J. Brunner, C. Schönenberger and M. Calame, *Nanotechnology*, 2012, **23**, 365201.
28 W. Haiss, C. S. Wang, I. Grace, A. S. Batsanov, D. J. Schiffrin, S. J. Higgins, M. R. Bryce, C. J. Lambert and R. J. Nichols, *Nat. Mater.*, 2006, **5**, 995–1002.
29 L. H. Yu, Z. K. Keane, J. W. Ciszek, L. Cheng, M. P. Stewart, J. M. Tour and D. Natelson, *Phys. Rev. Lett.*, 2004, **93**, 266802.
30 T. Taychatanapat, K. I. Bolotin, F. Kuemmeth and D. C. Ralph, *Nano Lett.*, 2007, **7**, 652–656.
31 N. P. de Leon, W. Liang, Q. Gu and H. Park, *Nano Lett.*, 2008, **8**, 2963–2967.
32 A. Salomon, D. Cahen, S. Lindsay, J. Tomfohr, V. B. Engelkes and C. D. Frisbie, *Adv. Mater.*, 2003, **15**, 1881–1890.
33 Z. L. Peng, Z. B. Chen, X. Y. Zhou, Y. Y. Sun, J. H. Liang, Z. J. Niu, X. S. Zhou and B. W. Mao, *J. Phys. Chem. C*, 2012, **116**, 21699–21705.
34 S. Wu, M. T. Gonzalez, R. Huber, S. Grunder, M. Mayor, C. Schonenberger and M. Calame, *Nat. Nanotechnol.*, 2008, **3**, 569–574.
35 L. Venkataraman, Y. S. Park, A. C. Whalley, C. Nuckolls, M. S. Hybertsen and M. L. Steigerwald, *Nano Lett.*, 2007, **7**, 502–506.
36 K. Baheti, J. A. Malen, P. Doak, P. Reddy, S. Y. Jang, T. D. Tilley, A. Majumdar and R. A. Segalman, *Nano Lett.*, 2008, **8**, 715–719.
37 W. Haiss, H. van Zalinge, S. J. Higgins, D. Bethell, H. Hobenreich, D. J. Schiffrin and R. J. Nichols, *J. Am. Chem. Soc.*, 2003, **125**, 15294–15295.
38 Z. H. Li, I. Pobelov, B. Han, T. Wandlowski, A. Blaszczyk and M. Mayor, *Nanotechnology*, 2007, **18**, 044018.
39 W. J. Liang, M. P. Shores, M. Bockrath, J. R. Long and H. Park, *Nature*, 2002, **417**, 725–729.
40 E. Leary, S. J. Higgins, H. van Zalinge, W. Haiss, R. J. Nichols, S. Nygaard, J. O. Jeppesen and J. Ulstrup, *J. Am. Chem. Soc.*, 2008, **130**, 12204–12205.
41 X. Y. Xiao, D. Brune, J. He, S. Lindsay, C. B. Gorman and N. J. Tao, *Chem. Phys.*, 2006, **326**, 138–143.
42 F. Li, J. Cheng, X. Chai, S. Jin, X. Wu, G.-A. Yu, S. H. Liu and G. Z. Chen, *Organometallics*, 2011, **30**, 1830–1837.
43 C. Li, A. Mishchenko, Z. Li, I. Pobelov, T. Wandlowski, F. Wurthner, A. Bagrets and F. Evers, *J. Phys.: Condens. Matter*, 2008, **20**, 374122.

44 Q. J. Chi, O. Farver and J. Ulstrup, *Proc. Natl. Acad. Sci. U. S. A.*, 2005, **102**, 16203–16208.
45 E. A. Della Pia, Q. J. Chi, J. E. Macdonald, J. Ulstrup, D. D. Jones and M. Elliott, *Nanoscale*, 2012, **4**, 7106–7113.
46 S. A. Getty, C. Engtrakul, L. Wang, R. Liu, S.-H. Ke, H. U. Baranger, W. Yang, M. S. Fuhrer and L. R. Sita, *Phys. Rev. B: Condens. Matter Mater. Phys.*, 2005, **71**, 241401.
47 Q. Lu, C. Yao, X. Wang and F. Wang, *J. Phys. Chem. C*, 2012, **116**, 17853–17861.
48 H. M. Wen, Y. Yang, X. S. Zhou, J. Y. Liu, D. B. Zhang, Z. B. Chen, J. Y. Wang, Z. N. Chen and Z. Q. Tian, *Chem. Sci.*, 2013, **4**, 2471–2477.
49 S. Jin, X. B. Jin, D. H. Wang, G. Z. Cheng, L. Peng and G. Z. Chen, *J. Phys. Chem. B*, 2005, **109**, 10658–10667.
50 Z. H. Li, Y. Q. Liu, S. F. L. Mertens, I. V. Pobelov and T. Wandlowski, *J. Am. Chem. Soc.*, 2010, **132**, 8187–8193.
51 E. D. Mentovich, N. Rosenberg-Shraga, I. Kalifa, M. Gozin, V. Mujica, T. Hansen and S. Richter, *J. Phys. Chem. C*, 2013, **117**, 8468–8474.
52 C. B. Gorman, R. L. Carroll and R. R. Fuierer, *Langmuir*, 2001, **17**, 6923–6930.
53 R. A. Wassel, G. M. Credo, R. R. Fuierer, D. L. Feldheim and C. B. Gorman, *J. Am. Chem. Soc.*, 2004, **126**, 295–300.
54 S. Jin, D. Wang, X. Jin and G. Z. Chen, *ChemPhysChem*, 2004, **5**, 1623–1629.
55 X. S. Zhou, J. H. Liang, Z. B. Chen and B. W. Mao, *Electrochem. Commun.*, 2011, **13**, 407–410.
56 X. S. Zhou, Z. B. Chen, S. H. Liu, S. Jin, L. Liu, H. M. Zhang, Z. X. Xie, Y. B. Jiang and B. W. Mao, *J. Phys. Chem. C*, 2008, **112**, 3935–3940.
57 S. Martin, W. Haiss, S. J. Higgins and R. J. Nichols, *Nano Lett.*, 2010, **10**, 2019–2023.
58 F. Chen, X. L. Li, J. Hihath, Z. F. Huang and N. J. Tao, *J. Am. Chem. Soc.*, 2006, **128**, 15874–15881.
59 X. L. Li, J. He, J. Hihath, B. Q. Xu, S. M. Lindsay and N. J. Tao, *J. Am. Chem. Soc.*, 2006, **128**, 2135–2141.
60 C. Li, I. Pobelov, T. Wandlowski, A. Bagrets, A. Arnold and F. Evers, *J. Am. Chem. Soc.*, 2008, **130**, 318–326.
61 X. Y. Zhou, Z. L. Peng, Y. Y. Sun, L. N. Wang, Z. J. Niu and X. S. Zhou, *Nanotechnology*, 2013, **24**, 465204.
62 J. Hihath and N. Tao, *Nanotechnology*, 2008, **19**, 265204.
63 M. L. Bai, J. H. Liang, L. Q. Xie, S. Sanvito, B. W. Mao and S. M. Hou, *J. Chem. Phys.*, 2012, **136**, 104701.
64 J. M. Soler, E. Artacho, J. D. Gale, A. García, J. Junquera, P. Ordejón and D. Sánchez-Portal, *J. Phys.: Condens. Matter*, 2002, **14**, 2745.
65 S. Martin, W. Haiss, S. Higgins, P. Cea, M. C. Lopez and R. J. Nichols, *J. Phys. Chem. C*, 2008, **112**, 3941–3948.
66 E. Leary, S. J. Higgins, H. van Zalinge, W. Haiss and R. J. Nichols, *Chem. Commun.*, 2007, 3939–3941.
67 W. Haiss, H. van Zalinge, H. Hobenreich, D. Bethell, D. J. Schiffrin, S. J. Higgins and R. J. Nichols, *Langmuir*, 2004, **20**, 7694–7702.
68 H. B. Michaelson, *J. Appl. Phys.*, 1977, **48**, 4729–4733.
69 I. V. Pobelovt, Z. H. Li and T. Wandlowski, *J. Am. Chem. Soc.*, 2008, **130**, 16045–16054.